

Nonholonomic Robot Stabilization by Vision-based Time-varying Controls

Dimitris P. Tsakiris *

Institute of Computer Science (ICS) - FORTH

Vassilika Vouton, P.O.Box 1385

71110 Heraklion, Crete, Greece

phone: +3081 391708, fax: +3081 391601

tsakiris@ics.forth.gr

<http://www.ics.forth.gr/~tsakiris>

Abstract

Docking or parallel parking maneuvers of mobile manipulators with nonholonomic constraints, guided by vision sensory data, are considered. This corresponds to the stabilization of a highly nonlinear system to a desired pose, for which time-varying state feedback controls are employed, using a vision-based approximation of the system's state. The vision data are provided by a camera carried by the arm of the mobile manipulator, which tracks a target of reference, as the robot moves. Two approaches are considered: the first involves continuous homogeneous time-varying controls, where the state information is updated at frame rate from vision. In order to improve robustness with respect to modeling errors, a second approach is explored, namely hybrid time-varying controls involving a combination of open- and closed-loop phases, where the state information is updated from vision data only at the beginning of each period of the periodic open-loop controls.

The experimental evaluation of the proposed techniques employs a nonholonomic mobile manipulator prototype developed in the robotics laboratory of INRIA Sophia-Antipolis, which offers the possibility of testing image understanding and control schemes in real-time on a dedicated multiprocessor system. The sensory apparatus of this robot is only crudely calibrated, hence our interest in control laws robust to modeling errors.

*Joint work with Claude Samson, Projet Icare, INRIA Sophia-Antipolis, France

Contents

1	Introduction	3
2	Modeling	5
2.1	Mobile Manipulator Kinematics	5
2.2	Vision Model	6
2.3	The Full System	7
3	Continuous Homogeneous Time-varying Controls	8
3.1	Mobile Platform Pose Stabilization	9
3.2	Manipulator Arm Control	10
3.3	Experiments	11
4	Hybrid Time-varying Controls	12
4.1	Robustness to Model Parameters	12
4.2	Mobile Manipulator Pose Stabilization	14
4.3	Experiments	14
5	Conclusion	16

1 Introduction

Sensor-based control strategies for robotic systems are well developed for manipulator arms; visual-servoing, for instance, which consists in the direct use of visual feedback in a system's control loop, (c.f. [7], [8], [9]), provides relatively simple and robust solutions to various positioning and tracking tasks. Their extension to the case of mobile robots is of significant importance for practical applications (e.g. in automating the docking maneuvers of AGVs in a manufacturing environment or the parallel parking maneuvers of cars). However, it becomes complicated by the presence of nonholonomic kinematic constraints, necessitating the use of more sophisticated nonlinear control tools.

We consider here the problem of exponential stabilization to a desired pose (position and orientation) of a mobile manipulator composed of a nonholonomic wheeled unicycle-type vehicle on which a holonomic manipulator arm is mounted. Localization of the mobile manipulator relative to its environment is achieved using visual data issued from a camera mounted at the tip of the manipulator arm. The nonholonomic constraints arise in the present case from the rolling-without-slipping of the robot's wheels on the plane supporting the system and constrain its instantaneous motion, whose component lateral to the heading direction is zero. Previous work on this problem by Pissard-Gibollet and Rives [20] attempted a direct extension of the holonomic visual-servoing approach: this achieved successful positioning of the camera with respect to its environment, but not positioning of the mobile platform of the system to a final desired position and orientation. Stabilization of the nonholonomic mobile platform is, however, the core problem. Moreover, point stabilization for such systems is, from the nonlinear control perspective, a harder problem than trajectory tracking ([6]) and, since most previous work on sensor-based control of mobile robots deals with trajectory tracking problems, this justifies our interest in this stabilization problem.

Systems of this type can be modeled as drift-free controllable affine nonlinear systems with fewer controls than states. Not only the linearization of these systems is uncontrollable, but also there do not exist continuous feedback control laws, involving only the state, that would asymptotically stabilize the system to an equilibrium. This is due to a topological obstruction pointed out by Brockett [3]. One of the approaches developed to solve the stabilization problem is the use of time-varying state feedback, i.e. control laws that depend explicitly, not only on the state, but also on time, usually in a periodic way. Samson [25] introduced them in the context of the unicycle point stabilization problem. Both the existence of continuous time-periodic stabilizing feedback controls for a wide class of systems (Coron [4]) and systematic procedures for the construction of smooth asymptotic stabilizers (Pomet [21], Morin, Pomet and Samson [17]) have been developed. As noted in Samson [25], smooth time-varying feedback controllers stabilize the system, but convergence to the desired equilibrium is only polynomial, not exponential. In fact, Lipschitz feedback can be shown to be unable to achieve exponential stabilization (M'Closkey and Murray [14]). However, Coron [5] established the existence of continuous only, time-varying controls, which stabilize the system in finite time and are smooth everywhere, except at the desired equilibrium. This leads to the existence of continuous time-varying controllers, which achieve a particular type of exponential stabilization (not exactly the classical one). M'Closkey and Murray [14] and Pomet and Samson [22] derived continuous non-Lipschitz homogeneous time-varying

exponentially stabilizing controls, which make the closed-loop system homogeneous of degree zero. Morin and Samson [15], [16] improved the design of controllers of this class, by providing ways of achieving a prespecified rate of exponential stabilization.

The implementation of a closed-loop control scheme, such as the one above, for accurate positioning and stabilization of the mobile manipulator to a desired configuration, depends upon our ability to estimate the state of the mobile robot at every time instant. This state estimation may rely on the use of absolute positioning devices or, as in the present instance, on the use of exteroceptive sensors (ultrasonic/infrared/vision sensors, laser range finders, etc.) for relative positioning with respect to environmental features.

The recovery of state information from sensory data requires appropriate models of the sensory and mechanical apparatus, whose parameters, however, are often imperfectly known due to, e.g. poor calibration of the system. This introduces unmodeled dynamics, which may destroy the stability of the closed-loop system. As shown by Hermes [10], Kawski [12], and Rosier [23], homogeneous exponentially stabilizing controls have some robustness properties with respect to additive perturbations of degree of homogeneity greater than that of the closed-loop system, but often this is not enough. Robustness with respect to a more general class of additive perturbations is examined by Bennani and Rouchon [2] and Morin and Samson [18] and leads to hybrid time-varying stabilizers consisting of consecutive open- and closed-loop phases. These stabilizers use open-loop steering of the system to the origin, which is periodically updated by state information at discrete time instants. Between two such time instants, the part of the controls that depends on the state is constant, but the controls themselves are not.

Both the continuous homogeneous and the hybrid time-varying exponentially stabilizing controls are applied to the mobile platform of our system, which is also equipped with a vision sensor mounted at the tip of the manipulator arm. The extra degrees-of-freedom associated with the arm make it possible to position the end-effector (and thus the camera) independently from the mobile platform. In this way, the camera can be made to track a target of interest (c.f. Aloimonos and Tsakiris [1], Papanikolopoulos, Khosla and Kanade [19] and the references on tracking surveyed in [8]), while the nonholonomic mobile platform performs the maneuvers necessary to its own positioning.

For simplicity, we only consider the planar case, where a mobile platform of the unicycle type carries an n -degree-of-freedom planar manipulator arm, with a camera that moves parallel to the plane supporting the mobile robot. Similarly, we only consider the kinematic model of the mobile robot, which is sufficient to handle the problems due to the nonholonomic constraints. A more detailed treatment of modeling, of real-time control architecture and of the control via continuous homogeneous time-varying exponential stabilizers appears in [26], [27], [28] and the references there.

In section 2, the kinematics and vision system of a nonholonomic mobile manipulator with an n -d.o.f. planar arm are modeled. In section 3, the vision-based control scheme using continuous homogeneous time-varying stabilizers for the mobile platform is presented, together with related experimental results. In section 4, the vision-based control scheme using hybrid time-varying stabilizers for the mobile platform, as well as some recent related experimental results, are detailed.

2 Modeling

2.1 Mobile Manipulator Kinematics

We consider a mobile robot of the unicycle type carrying an n -d.o.f. planar manipulator arm with a camera mounted on its end effector (figure 1 shows the case of $n = 3$).

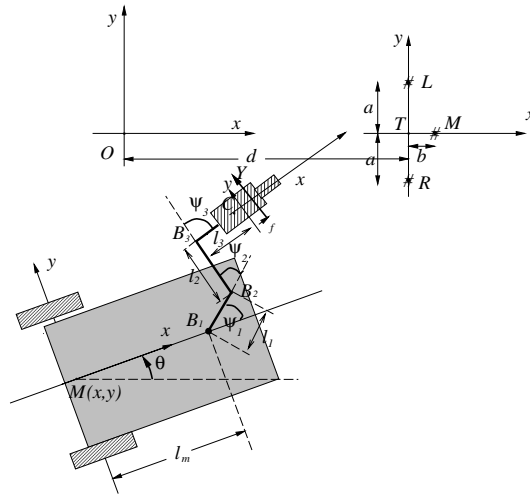


Figure 1: Mobile Manipulator with Camera

Consider an inertial coordinate system $\{F_O\}$ centered at a point O of the plane, a moving coordinate system $\{F_M\}$ attached to the middle M of the robot's wheel axis and another moving one $\{F_C\}$ attached to the optical center C of the camera. Let (x, y) be the position of the point M and θ be the orientation of the mobile robot with respect to the coordinate system $\{F_O\}$; let l_m be the distance of the point M from the first joint B_1 of the n -d.o.f. planar arm, with l_1, \dots, l_n being the lengths of the links of the arm and ψ_1, \dots, ψ_n being its joint coordinates.

Let $(x_{MC}, y_{MC}, \theta_{MC})$ represent the configuration of $\{F_C\}$ with respect to $\{F_M\}$, $(x_{CT}, y_{CT}, \theta_{CT})$ represent the configuration of $\{F_T\}$ with respect to $\{F_C\}$, (x_C, y_C, θ_C) represent the configuration of $\{F_C\}$ with respect to $\{F_O\}$ and (x_T, y_T, θ_T) represent the configuration of $\{F_T\}$ with respect to $\{F_O\}$, where $x_T = d$ is the distance of point T from point O and $y_T = \theta_T = 0$.

From the kinematic chain of figure 1, we have for the case of an n -degree-of-freedom manipulator arm:

$$\begin{aligned} \theta_C &= \theta + \sum_{i=1}^n \psi_i, & x_C &= x + l_m \cos \theta + \sum_{i=1}^n l_i \cos \left(\theta + \sum_{j=1}^i \psi_j \right), \\ y_C &= y + l_m \sin \theta + \sum_{i=1}^n l_i \sin \left(\theta + \sum_{j=1}^i \psi_j \right). \end{aligned} \tag{1}$$

Velocity Kinematics: By differentiating the chain kinematics of the mobile manipulator and its environment, assuming that we consider stationary targets and solving for the spatial velocity of the target frame with respect to the camera frame Ξ^{CT} , we get

$$\Xi^{CT} \stackrel{\text{def}}{=} \begin{pmatrix} \dot{x}_{CT} + \dot{\theta}_{CT} y_{CT} \\ \dot{y}_{CT} - \dot{\theta}_{CT} x_{CT} \\ \dot{\theta}_{CT} \end{pmatrix} = \begin{pmatrix} B_{1,1} & B_{1,2} \end{pmatrix} \begin{pmatrix} \dot{\mathcal{X}} \\ \dot{q} \end{pmatrix}, \quad (2)$$

where $\mathcal{X} \stackrel{\text{def}}{=} (x, y, \theta)^\top$ is the state of the mobile robot, while $q \stackrel{\text{def}}{=} (\psi_1, \psi_2, \dots, \psi_n)^\top$ is the configuration of the manipulator arm and where the matrix $B_{1,1}$ is

$$\begin{pmatrix} -\cos \theta_C & -\sin \theta_C & b_1^{1,1} \\ \sin \theta_C & -\cos \theta_C & b_2^{1,1} \\ 0 & 0 & -1 \end{pmatrix}, \quad (3)$$

with θ_C given by equation 1, $b_1^{1,1} \stackrel{\text{def}}{=} -l_m \sin(\sum_{i=1}^n \psi_i) - \sum_{i=1}^{n-1} l_i \sin(\sum_{j=i+1}^n \psi_j)$, $b_2^{1,1} \stackrel{\text{def}}{=} -l_m \cos(\sum_{i=1}^n \psi_i) - \sum_{i=1}^{n-1} l_i \cos(\sum_{j=i+1}^n \psi_j) - l_n$ and with the $3 \times n$ matrix $B_{1,2}$, being the Jacobian of the manipulator arm.

Nonholonomic Constraints: The nonholonomic constraints on the motion of the mobile robot arise from the rolling-without-slipping of the mobile platform's wheels on the plane supporting the system. Due to these constraints, the instantaneous velocity lateral to the heading direction of the mobile platform has to be zero.

From this we get the usual unicycle kinematic model for the mobile platform:

$$\dot{x} = v \cos \theta, \quad \dot{y} = v \sin \theta, \quad \dot{\theta} = \omega, \quad (4)$$

where $v \stackrel{\text{def}}{=} \dot{x} \cos \theta + \dot{y} \sin \theta$ is the heading speed and ω is the angular velocity of the unicycle. Then

$$\dot{\mathcal{X}} = B_{3,1}(X) \begin{pmatrix} v \\ \omega \end{pmatrix} = \begin{pmatrix} \cos \theta & 0 \\ \sin \theta & 0 \\ 0 & 1 \end{pmatrix} \begin{pmatrix} v \\ \omega \end{pmatrix}. \quad (5)$$

2.2 Vision Model

Consider a target containing three easily identifiable feature points arranged in the configuration of figure 1. The coordinates of the three feature points with respect to $\{F_T\}$ are $(x_p^{\{T\}}, y_p^{\{T\}})$, $p \in \{l, m, r\}$. The distances a and b (fig. 1) are assumed to be known. The coordinates of the feature points with respect to the camera coordinate frame $\{F_C\}$ can be easily found.

We assume the usual pinhole camera model for our vision sensor, with perspective projection of the target's feature points (viewed as points on the plane \mathbb{R}^2) on a 1-dimensional image plane (analogous to a linear CCD array). This defines the projection function \mathcal{P} of a point of \mathbb{R}^2 , which has coordinates (x, y) with respect to the camera coordinate frame $\{F_C\}$, as

$$\mathcal{P} : \mathbb{R}_+ \times \mathbb{R} \longrightarrow \mathbb{R} : (x, y) \longmapsto \mathcal{P}(x, y) = f \frac{y}{x}. \quad (6)$$

where f is the focal length of the camera. In our setup, the coordinate x corresponds to “depth”.

Let the projections of the target feature points on the image plane be $Y_p = \mathcal{P}(x_p^{\{C\}}, y_p^{\{C\}})$, $p \in \{l, m, r\}$, given by 6. The vision data are then $Y_v \stackrel{\text{def}}{=} (Y_l, Y_m, Y_r)^\top$. Differentiating 6, we get the well-known equations of the optical flow [11] for the 1-dimensional case:

$$\dot{Y}_v = B_{2,1}(Y_p, x_p^{\{C\}}) \Xi^{CT} = \begin{pmatrix} -\frac{1}{x_l^{\{C\}}} Y_l & \frac{1}{x_l^{\{C\}}} f & \frac{1}{f}(f^2 + Y_l^2) \\ -\frac{1}{x_m^{\{C\}}} Y_m & \frac{1}{x_m^{\{C\}}} f & \frac{1}{f}(f^2 + Y_m^2) \\ -\frac{1}{x_r^{\{C\}}} Y_r & \frac{1}{x_r^{\{C\}}} f & \frac{1}{f}(f^2 + Y_r^2) \end{pmatrix} \Xi^{CT}, \quad (7)$$

where the matrix $B_{2,1}(Y_p, x_p^{\{C\}})$ corresponds to the Jacobian of the visual data, the so-called *interaction matrix* [7], [8], [9].

2.3 The Full System

The above modeling equations of the mobile robot with the n -d.o.f. manipulator arm can be regrouped to derive a few basic relations.

The state of the system is $X = (\mathcal{X}, q)^\top$. The velocity kinematics gives

$$\begin{pmatrix} \Xi^{CT} \\ \dot{q} \end{pmatrix} = B_1(X) \dot{X} = \begin{pmatrix} B_{1,1} & B_{1,2} \\ \mathbf{0}_{n \times 3} & \mathbb{I}_{n \times n} \end{pmatrix} \begin{pmatrix} \dot{\mathcal{X}} \\ \dot{q} \end{pmatrix}. \quad (8)$$

The sensory data are $Y = (Y_v, q)^\top$. The optical flow equations give

$$\dot{Y} = B_2(X) \begin{pmatrix} \Xi^{CT} \\ \dot{q} \end{pmatrix} = \begin{pmatrix} B_{2,1} & \mathbf{0}_{3 \times n} \\ \mathbf{0}_{n \times 3} & \mathbb{I}_{n \times n} \end{pmatrix} \begin{pmatrix} \Xi^{CT} \\ \dot{q} \end{pmatrix}. \quad (9)$$

The relationship between the state and the sensory data is $Y = \Phi(X)$. The corresponding differential relationship is given by equations 8 and 9:

$$\dot{Y} = \frac{\partial \Phi}{\partial X}(X) \dot{X} = B_2(X) B_1(X) \dot{X}. \quad (10)$$

The controls of the system are $\mathcal{U} = (v, \omega, \omega_{\psi_1}, \dots, \omega_{\psi_n})^\top = (v, \dot{\theta}, \dot{q})^\top$. Then

$$\dot{X} = \begin{pmatrix} \dot{\mathcal{X}} \\ \dot{q} \end{pmatrix} = B_3(X) \mathcal{U} = \begin{pmatrix} B_{3,1} & \mathbf{0}_{3 \times n} \\ \mathbf{0}_{n \times 2} & \mathbb{I}_{n \times n} \end{pmatrix} \begin{pmatrix} v \\ \dot{\theta} \\ \dot{q} \end{pmatrix}. \quad (11)$$

Due to the nonholonomic constraints, the dimension of the control space is strictly less than that of the state space ($\dim \mathcal{U} < \dim X$).

A more detailed discussion of the modeling aspects of this system can be found in [27], [28].

3 Continuous Homogeneous Time-varying Controls

Consider a mobile robot with only one actuated pan-axis. The system state is $X = (x, y, \theta, \psi_1)^\top$, the sensory data are $Y = (Y_l, Y_m, Y_r, \psi_1)^\top$ and the controls are $\mathcal{U} = (v, \omega, \omega_{\psi_1})^\top$. The problem that we consider is to stabilize the mobile platform to the desired configuration, which, without loss of generality, will be chosen to be zero, i.e. $X^* = (x^*, y^*, \theta^*, \psi_1^*) = 0$. The corresponding visual data $Y_v^* = (Y_l^*, Y_m^*, Y_r^*)$ can be directly measured by driving the system to the desired configuration or can be easily specified from the models, provided d is also known, along with the target geometry a and b (see figure 1).

An exponentially stabilizing control is considered for the mobile platform, while a control that keeps the targets foveated is considered for the camera. First, some notions of homogeneous systems are presented, related to their stability and robustness.

Homogeneous Systems: A *dilation* δ_ϵ^r is a function $\delta_\epsilon^r : \mathbb{R}^n \rightarrow \mathbb{R}^n$ defined as $\delta_\epsilon^r(x_1, \dots, x_n) = (\epsilon^{r_1}x_1, \dots, \epsilon^{r_n}x_n)$, for $\epsilon > 0$ and weights $r_i > 0$, $i = 1, \dots, n$.

A continuous function $f : \mathbb{R}^n \rightarrow \mathbb{R}$ is *homogeneous of degree m* with respect to the dilation δ_ϵ^r , if $f(\delta_\epsilon^r(x)) = \epsilon^m f(x)$, for all $\epsilon > 0$.

A continuous function $\rho : \mathbb{R}^n \rightarrow \mathbb{R}$ is called a *homogeneous norm* with respect to the dilation δ_ϵ^r , if i) $\rho(x) \geq 0$, ii) $\rho(x) = 0$ if and only if $x = 0$, and iii) if it is homogeneous of degree one, i.e. $\rho(\delta_\epsilon^r(x)) = \epsilon\rho(x)$, for all $\epsilon > 0$. (Notice that the triangle inequality is not required.) A frequently used *homogeneous norm* associated to δ_ϵ^r is $\rho(x) = (\sum_{i=1}^n |x_i|^{\frac{p}{r_i}})^{\frac{1}{p}}$, with $p > 0$.

A continuous vector field X on \mathbb{R}^n is *homogeneous of degree m* with respect to the dilation δ_ϵ^r , if X is expressed locally as $X(x) = \sum_{i=1}^n X_i(x) \frac{\partial}{\partial x_i}$, with $X_i(x)$ a homogeneous function of degree $r_i + m$.

For time-dependent systems, we still consider the above definitions, but with the dilation:

$$\delta_\epsilon^r(t, x_1, \dots, x_n) = (t, \epsilon^{r_1}x_1, \dots, \epsilon^{r_n}x_n). \quad (12)$$

The equilibrium $x = 0$ of the system $\dot{x} = f(t, x)$ is *locally exponentially stable* with respect to the homogeneous norm $\rho(\cdot)$ associated to the dilation δ_ϵ^r , if there is a neighborhood U of $x = 0$ and positive constants α and β such that $\rho(x(t)) \leq \alpha\rho(x(0))e^{-\beta t}$, for all $t \geq 0$ and $x(0) \in U$. If $U = \mathbb{R}^n$, the exponential stability of $x = 0$ is global.

Asymptotic stability is a robust property for homogeneous systems, in the sense that perturbations, which have a higher degree of homogeneity, do not destroy it. This was shown for autonomous systems by Hermes [10], Kawski [12] and Rosier [23] and was extended to time-varying periodic systems by Pomet and Samson [22] and M'Closkey and Murray [14] as follows:

Proposition 1 *Consider the system*

$$\dot{x} = f(t, x) \quad (13)$$

with $f(t, x) : \mathbb{R} \times \mathbb{R}^n \rightarrow \mathbb{R}^n$ a periodic continuous vector field of period T and with $f(t, 0) = 0$. Assume the system 13 is homogeneous of degree 0 with respect to the dilation δ_ϵ^r

in 12 and that the equilibrium $x = 0$ is locally asymptotically stable. Then, it is also globally exponentially stable in the above sense. Moreover, consider the perturbed system

$$\dot{x} = f(t, x) + g(t, x), \quad (14)$$

with $g(t, x) : \mathbb{R} \times \mathbb{R}^n \rightarrow \mathbb{R}^n$ a periodic continuous vector field with the same period T as before and which is the sum of homogeneous vector fields of degree strictly positive with respect to δ_c^r . The origin $x = 0$ of system 14 is locally exponentially stable.

3.1 Mobile Platform Pose Stabilization

Mobile platform control synthesis: In order to facilitate the synthesis of the controller for the mobile platform, a locally diffeomorphic transformation of the states and inputs is applied

$$(x_1, x_2, x_3)^\top \stackrel{\text{def}}{=} (x, y, \tan \theta)^\top, \quad u_1 = \cos \theta v, \quad u_2 = \frac{1}{\cos^2 \theta} \omega, \quad (15)$$

which brings the unicycle kinematics (eq. 4) in the so-called *chained form* [22], [15]:

$$\dot{x}_1 = u_1, \quad \dot{x}_2 = x_3 u_1, \quad \dot{x}_3 = u_2. \quad (16)$$

The mobile platform control, which can be used if the state is known or reconstructed, is given by:

$$v(t, X) = \frac{1}{\cos \theta} u_1(t, \Psi(X)), \quad \omega(t, X) = \cos^2 \theta u_2(t, \Psi(X)), \quad (17)$$

where u_1 and u_2 are the continuous time-varying state-feedback controls, developed by Morin and Samson [16] for the 3-dimensional 2-input chained-form system of equation 16. These controls, given in terms of the chained-form coordinates of equation 15, are:

$$\begin{aligned} u_1(t, x_1, x_2, x_3) &= -k_1 \alpha x_1 + k_1 \rho_3(x_2, x_3) \sin wt, \\ u_2(t, x_1, x_2, x_3) &= -\frac{k_3}{\rho_3(x_2, x_3)} \left[|u_1| x_3 + k_2 u_1 \frac{x_2}{\rho_3(x_2, x_3)} \right], \end{aligned} \quad (18)$$

where $\rho_3(x_2, x_3) \stackrel{\text{def}}{=} (|x_2|^2 + |x_3|^3)^{\frac{1}{6}}$, w is the frequency of the time-varying controls and α, k_1, k_2, k_3 are positive gains. The controls u_1 and u_2 are homogeneous of degree 1 and 2, respectively, with respect to the dilation with weights $r = (1, 3, 2)$, while the closed-loop chained-form system is homogeneous of degree zero. The exponential convergence to zero of the closed-loop system can be established using the homogeneous norm $\rho(x_1, x_2, x_3) \stackrel{\text{def}}{=} (|x_1|^6 + |x_2|^2 + |x_3|^3)^{\frac{1}{6}}$. The time-varying state feedback control \mathcal{U} for the mobile platform is then $\mathcal{U}(t, X) = (v(t, X), \omega(t, X))^\top$.

State Approximation: Such a control requires an estimate \hat{X} of the current state X of the system with respect to its desired configuration. This estimate can be provided by state reconstruction from the visual data. However, since we are interested in positioning the mobile robot to the desired configuration $X^* = 0$, while starting relatively close to it,

we could attempt to do so without reconstructing its state explicitly. Since $Y = \Phi(X)$, the state X can be approximated, near the desired configuration $X^* = 0$, up to first order by

$$\hat{X}(Y) = \left[\frac{\partial \Phi}{\partial X}(X^*) \right]^{-1} (Y - Y^*), \quad (19)$$

where $\frac{\partial \Phi}{\partial X} = B_2(X)B_1(X)$ with B_1 and B_2 as specified in 8 and 9. Equation 19 is proportional to the difference of the current visual data from their desired values and it only involves the Jacobian $\frac{\partial \Phi}{\partial X}$ evaluated at the desired configuration X^* , which can be determined either analytically from the models or experimentally. The proposed control law for the mobile platform can thus be expressed as a function of only the sensory data $\mathcal{U} = \mathcal{U}(t, Y)$.

3.2 Manipulator Arm Control

In order to implement a vision-based state-feedback control law for the mobile platform, we need to continuously observe the target during the motion of the platform. The arm control ω_{ψ_1} is chosen to keep the target foveated (at the center of the image plane), by regulating the angular deviation of the line-of-sight of the camera from the targets to zero, while the mobile platform moves. It is specified so that the distance of the middle target Y_m from its desired value Y_m^* is made to decrease exponentially by regulating the output function $e(X) \stackrel{\text{def}}{=} Y_m - Y_m^*$ to zero and by making the closed-loop system for e behave like $\dot{e} = -\lambda e$, for a positive gain λ . This is analogous to the task function approach to visual servoing [7], [24] and gives

$$\omega_{\psi_1}(t, X, Y) = -\frac{\lambda}{\mathcal{J}_{2,3}}(Y_m - Y_m^*) - \left(\frac{\mathcal{J}_{2,1}}{\mathcal{J}_{2,3}} v + \frac{\mathcal{J}_{2,2}}{\mathcal{J}_{2,3}} \omega \right), \quad (20)$$

where $\mathcal{J}_{2,i}$ is the $(2, i)$ -entry of the matrix $\mathcal{J}(X) \stackrel{\text{def}}{=} B_2(X) B_1(X) B_3(X)$. In particular, $\mathcal{J}_{2,3} = -f - \left(\frac{Y_m^2}{f} + \frac{l_2 f}{x_m^2(c_1)} \right)$. The first term of equation 20 makes the arm track the targets, while the term in parenthesis pre-compensates for the motion of the mobile platform. A useful simplification of this control law can be obtained by ignoring this pre-compensation term and by setting $\mathcal{J}_{2,3} \approx -f$. This approach can be extended to control mobile manipulators with arms of more than one degree-of-freedom [27], [28].

Vision data capture and processing introduces delays in the system, which manifest themselves by a deterioration of the controlled system's characteristics. In the case of the arm control in particular, they appear as an underdamped step response, which cannot be corrected by altering the gains of the control law. It can, however, be ameliorated by appropriate compensation using the mobile platform wheel and manipulator arm encoders, whose readings are readily available. Due to such a delay δ , the vision data used in the control law 20 are $Y_m(t - \delta)$, instead of $Y_m(t)$. However, $Y_m(t) - Y_m(t - \delta)$ can be approximated near X^* by a weighted sum of the encoder increments during the time interval $[t - \delta, t]$. Then, in equation 20, $Y_m(t) = Y_m(t - \delta) + [Y_m(t) - Y_m(t - \delta)]$, where the first term of the RHS comes from the vision data, while the term in brackets comes from the encoder increments.

3.3 Experiments

The control law presented above has been validated by experiments on a unicycle-type mobile robot carrying a 6-d.o.f. manipulator arm with a CCD camera ([26], [27]). Details on the real-time control architecture issues appear in [26].

In the experimental results presented below, the control law 17 is used, with the chained form system controls 18, the simplified version of the delay-compensated arm control 20 and the state approximation 19 by vision data. The controls are evaluated every time new sensory data become available, i.e. at frame rate (40 msec).

The controls 18 are normalized by reparametrizing their time dependence, so that the system's trajectory retains its qualitative characteristics (e.g. the number of switchings before getting close to zero, the maximum excursion in the x -direction), but a finer tuning of the magnitude of the controls becomes possible. This allows a better control of the time traversal of the trajectory and can be useful in avoiding actuator saturation, wheel sliding and the excitation of unmodeled dynamics. This normalization does not affect the exponential stabilization of the system, only its rate.

Initial experiments used the raw visual data to calculate the state and the controls. Implementation of such a scheme leads to significant oscillations and jerks during the motion of the system [27]. To fix this problem, subsequent experiments used filtering of each of the state variables (x, y, θ). This makes the corresponding trajectories smoother. No filtering was used on the visual data themselves. The resulting (x, y) -trajectory, as well as the corresponding controls v, ω are plotted in figure 2. In the (x, y) -plots, the dotted line represents data obtained by odometry, while the solid one represents data obtained by vision.

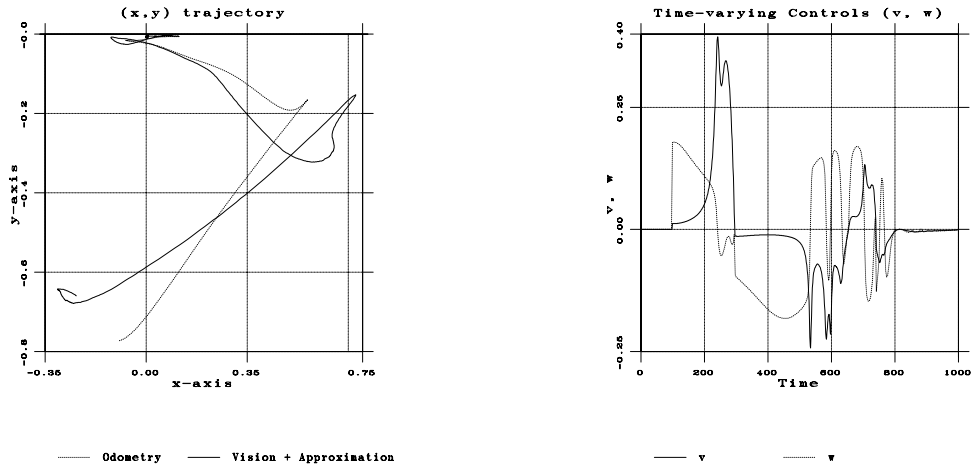


Figure 2: Mobile platform (x, y) -trajectory and controls v, ω

Figure 2 shows that the system gets near the origin after very few parallel-parking-type maneuvers. At this point, we test whether the system has reached a sufficiently small neighborhood of the origin and, then, the part of the controls that depend on the state y is set to zero. If it is not, the system will enter a limit cycle, as shown in fig. 3. In this figure, the left plot shows the (x, y) -trajectory of the system near the origin, as recorded by

odometry and the right plot shows the evolution of the states x , y , θ of the mobile platform. Although this limit cycle can be avoided in applications, as proposed earlier, it is of some theoretical interest, since it could be due to the poor robustness properties of the continuous homogeneous exponential stabilizers in the presence of unmodeled dynamics not belonging to the class of perturbations allowed by Proposition 1.

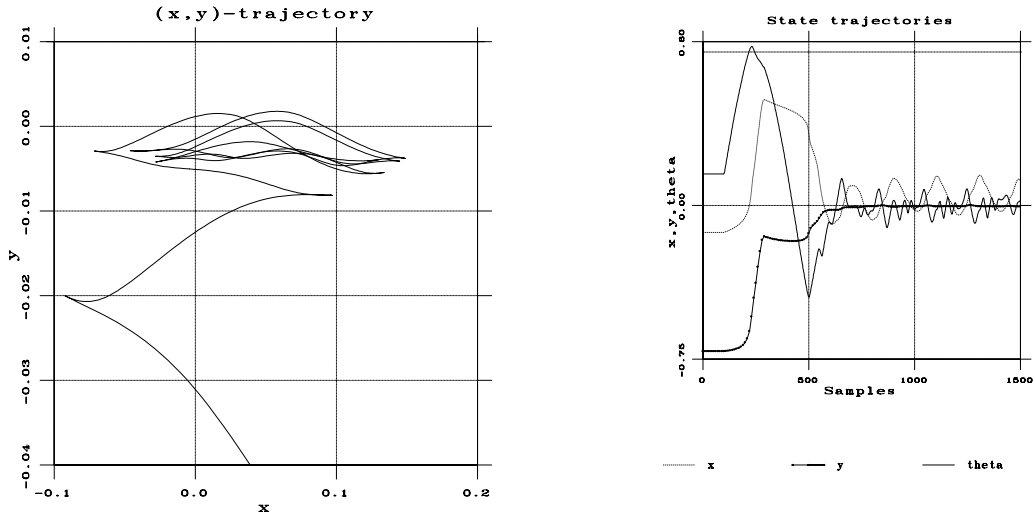


Figure 3: Mobile platform (x, y) -trajectory and states x , y , θ : Limit cycle

Some advantageous features of this control scheme, stemming from the feedback nature of the stabilizing controls, are the lack of a need for detailed planning of the system's trajectories and its reactivity to movements of the target which redefine the pose at which the system needs to be stabilized.

4 Hybrid Time-varying Controls

4.1 Robustness to Model Parameters

Consider the analytic affine driftless system on \mathbb{R}^n

$$\dot{x} = \sum_{i=1}^m f_i(x) u_i, \quad (21)$$

which is locally controllable around the origin. We would like to use feedback control laws that stabilize exponentially (as defined below) the origin of this system, as well as that of any perturbed system

$$\dot{x} = \sum_{i=1}^m [f_i(x) + h_i(\epsilon, x)] u_i, \quad (22)$$

for $|\epsilon|$ sufficiently small and with h_i analytic in $\mathbb{R} \times \mathbb{R}^n$ and $h_i(0, x) = 0$. These additive perturbation terms may correspond to modeling errors due to poor calibration of the system.

Continuous homogeneous time-varying exponential stabilizers, like the ones derived in [14], [15], [16] and those used in section 3, are not robust in this sense (as shown by

Lizarraga, Morin and Samson [13]), even though they are robust with respect to less general unmodeled dynamics, as shown in Proposition 1.

The robust control laws derived by Morin and Samson [18] and used in our experiments consist in applying periodic open-loop controls steering the system to the origin, which are continuous with respect to state initial conditions and where the state information is only updated at the beginning of each period of the controls. In order to define the sense in which these control laws stabilize the systems 21 and 22, the following system is appended to each of them, to form an extended system:

$$\dot{y} = \left(\sum_{k \in \mathbb{N}} \delta_{kT} \right) (x - y_{-\alpha}) , \quad (23)$$

for $0 < \alpha < T$, with T the period of the controls, δ_{kT} the Dirac impulse at time kT and $y_{-\alpha}$ the delay operator such that $y_{-\alpha}(t) = y(t - \alpha)$. This extra system indicates that $y(t)$ is constant and equal to $x(kT)$ on the time interval $[kT, (k + 1)T)$. Thus, any control, which, during this interval, is a function of only $x(kT)$ and t , can be interpreted as a control $u(y, t)$ for the corresponding extended system. A feedback control $u(x, y, t)$ is an exponential stabilizer for the extended systems above, if there exists an open set $U \in \mathbb{R}^n \times \mathbb{R}^n$ containing the point $(0, 0)$, a real $\gamma > 0$ and a function β of class \mathcal{K} , such that the solutions $(x(t), y(t))$ of the controlled system satisfy

$$\|(x(t), y(t))\| \leq \beta(\|(x(t_0), y(t_0))\|) \exp(-\gamma(t - t_0)) , \quad (24)$$

for every $t \geq t_0 \geq 0$ and for every $(x(t_0), y(t_0)) \in U$, where $\|\cdot\|$ is the Euclidean norm in \mathbb{R}^n .

The order notation is used in the sequel, where $o(x)$ denotes a function such that $\frac{\|o(x)\|}{\|x\|} \rightarrow 0$ as $\|x\| \rightarrow 0$, while $O(x)$ denotes a function such that $\frac{\|O(x)\|}{\|x\|} \leq K$, for some $K > 0$ and for x in some neighborhood of the origin.

The following result of Morin and Samson [18] provides sufficient conditions for a control $u(y, t)$ to robustly exponentially stabilize the origin of the nominal extended system.

Proposition 2 *Consider the analytical locally controllable system of equation 21, a neighborhood U of the origin of \mathbb{R}^n and a function $u \in \mathcal{C}^0(U \times [0, T]; \mathbb{R}^m)$. Assume that*

1. *there exist $\alpha, K > 0$ such that $\|u(x, t)\| \leq K \|x\|^\alpha$, for all $(x, t) \in U \times [0, T]$,*
2. *the solution $x(\cdot)$ of*

$$\dot{x} = \sum_{i=1}^m f_i(x) u_i(x_0, t) , \quad (25)$$

with $x(0) = x_0 \in U$, satisfies $x(T) = A x_0 + o(x_0)$, where A is a discrete-stable matrix (i.e. all its eigenvalues are strictly inside the complex unit circle).

3. *for any vector of ordered indices $I = (i_1, \dots, i_k)$, with $k \in \mathbb{N}_+$ and i_1, \dots, i_k integers from the set $\{1, \dots, m\}$ (possibly with repetitions), with length $|I| \leq \frac{1}{\alpha}$, the following holds (this assumption is only needed when $\alpha < 1$):*

$$\int_0^T \int_0^{t_k} \cdots \int_0^{t_2} u_{i_k}(x, t_k) u_{i_{k-1}}(x, t_{k-1}) \cdots u_{i_1}(x, t_1) dt_1 \cdots dt_k = O(x) . \quad (26)$$

Then, given the family of perturbed systems of equation 22, there exists $\epsilon_0 > 0$, such that the origin of the corresponding extended systems (equations 22 and 23) is locally exponentially stabilized by the control $u(y, t)$ for any $\epsilon \in (-\epsilon_0, \epsilon_0)$.

4.2 Mobile Manipulator Pose Stabilization

Consider the 3–dimensional 2–input chained–form system of equation 16 and the corresponding perturbed system with additive perturbations of the type of equation 22. Consider the sinusoidal control law

$$u_1(t, x) = -\frac{x_1}{T} + w \rho_1(x) \sin wt, \quad u_2(t, x) = -\frac{x_3}{T} - \frac{2}{T} \frac{x_2}{\rho_1(x)} \cos wt, \quad (27)$$

where $T = \frac{2\pi}{w}$ is the period of the controls and $\rho_1(x) \stackrel{\text{def}}{=} \frac{1}{2}\sqrt{|x_2|}$.

It is possible to verify that this control law satisfies the assumptions of Proposition 2. Indeed, consider the dilation with weights $r = (1, 2, 1)$. The norm ρ_1 is homogeneous with respect to this dilation, while both controls u_1 and u_2 are homogeneous of degree 1 and the closed–loop system 16 is homogeneous of degree zero. Thus, assumption 1 is verified with $\alpha = \frac{1}{\max r_i} = \frac{1}{2}$.

Assuming that the systems starts at $x(0)$ and by integrating the closed–loop system of equation 16 with the control law $u_1(t, x(0)), u_2(t, x(0))$ over the time interval $[0, T]$, we get

$$x_1(T) = 0, \quad x_2(T) = \frac{1}{2}[\sqrt{|x_2(0)|} - x_1(0)]x_3(0), \quad x_3(T) = 0. \quad (28)$$

It is easy to see that this satisfies assumption 2 with $A = 0_{3 \times 3}$, which is discrete–stable. Observe that for a generic $x(0)$ and under this control law, the system does not reach the origin in one step. This, however, is not necessary for its convergence to the origin.

In order to check assumption 3, one needs to check condition 26 over all vectors of indices I of length $|I| \leq \frac{1}{\alpha} = 2$, with indices belonging to the set $\{1, 2\}$. The following vectors need, then, to be considered: (1), (2), (1, 1), (1, 2), (2, 1) and (2, 2). Evaluation of the corresponding integrals gives:

$$\begin{aligned} \int_0^T u_1(t_1, x) dt_1 &= -x_1, \quad \int_0^T u_2(t_1, x) dt_1 = -x_3, \\ \int_0^T \int_0^{t_2} u_1(t_2, x) u_1(t_1, x) dt_1 dt_2 &= \frac{1}{2}x_1^2, \\ \int_0^T \int_0^{t_2} u_1(t_2, x) u_2(t_1, x) dt_1 dt_2 &= -x_2 + \frac{1}{2}[\sqrt{|x_2|} - x_1]x_3, \\ \int_0^T \int_0^{t_2} u_2(t_2, x) u_1(t_1, x) dt_1 dt_2 &= x_2 - \frac{1}{2}[\sqrt{|x_2|} - x_1]x_3, \\ \int_0^T \int_0^{t_2} u_2(t_2, x) u_2(t_1, x) dt_1 dt_2 &= \frac{1}{2}x_3^2. \end{aligned} \quad (29)$$

In all these cases, assumption 3 is satisfied. Thus, the control $u(t, x(kT))$, for $t \in [kT, (k+1)T)$ of equation 27 is a robust exponential stabilizer for the 3–dimensional 2–input chained–form system.

The corresponding control for the unicycle is obtained as described in section 3.1 (equations 17 and 18) and the manipulator arm is controlled as described in section 3.2. The approximation of the state from the visual data, which provides the state estimates $x(kT)$ at the beginning of each new period of the controls, is done as described in section 3.1.

4.3 Experiments

The experimental apparatus described in section 3.3 was appropriately adapted to the application of the hybrid time–varying stabilizers described above. The (x, y) –trajectory of the

mobile manipulator resulting from the application of the use of this control law is shown in fig. 4. The corresponding controls are shown in the right plot of this figure (the solid line is v and the dotted one is ω).

The control law 27 produces abrupt angular velocity transitions at the beginning of each new period (due to the $\cos wt$ term), which result in significant jerks of the mobile platform. In order to ameliorate this, the $\cos wt$ was replaced by $\cos wt - \cos 2wt$.

A method for compensating the vision-induced delays was presented in section 3.2. This, however, assumes that the delay is exactly known, which may be hard to estimate. The present control law makes an alternative approach possible, namely to stop the system at the end of each period of the controls for sufficiently long to overcome the vision system delays. Then, the vision data, which will be used at the beginning of the next period of the controls to estimate the state, reflect the current state of the system.

The control law is evaluated at intervals of 15 msec and is normalized as discussed in section 3.3. Normalization of the controls alters their temporal characteristics, in particular the period T . The detection of the beginning of a new period, at which point the new state estimate will be applied, becomes an issue. This detection is implemented by identifying the time instant at which $\sin wt$ changes from a negative value to a positive one, while $\cos wt$ is positive. There will, however, always be an imprecision in the identification of this time instant, which is related to the discretization of the control law. As remarked in [18], this can result in a degradation of the performance of this class of controllers. This may explain the persistence of a limit cycle (fig. 5), although of one of reduced size compared to the limit cycle produced by the continuous homogeneous control law.

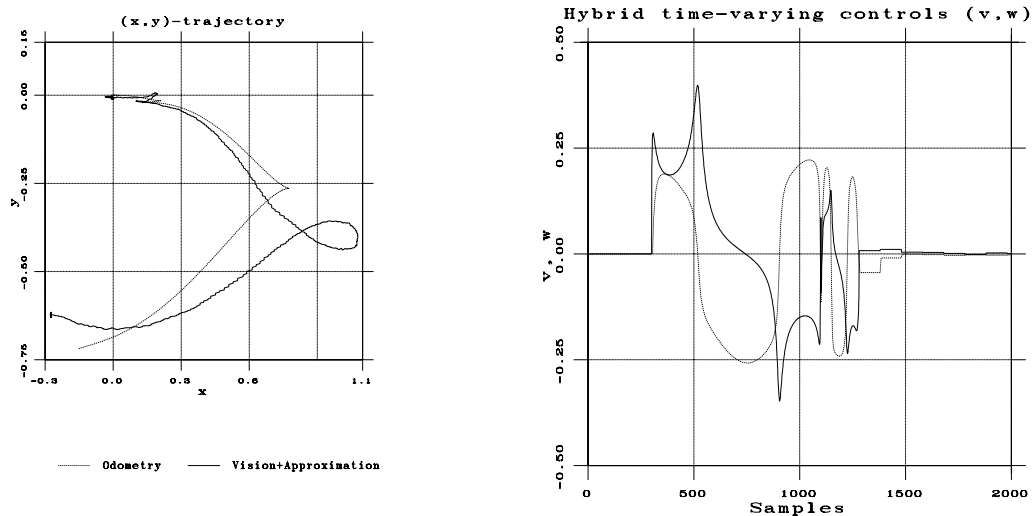


Figure 4: Mobile platform (x, y) -trajectory and controls v, ω

This control scheme retains the advantages of the one in section 3 related to planning of trajectories and to reactivity with respect to movements of the target. This reactivity, however, will now appear only when the visual data are used by the control law, i.e. at the beginning of a new period of the controls, and not during their open-loop phase.

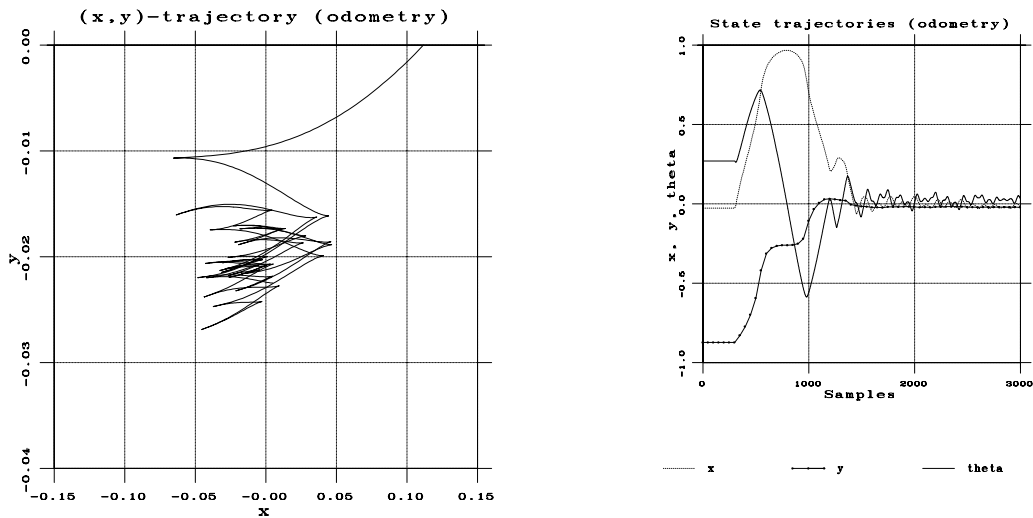


Figure 5: Mobile platform (x, y) -trajectory and states x, y, θ : Limit cycle

5 Conclusion

Several schemes for sensor-based control of a nonholonomic mobile manipulator were presented. These constitute the first, to our knowledge, detailed evaluation of time-varying stabilizing controls when exteroceptive sensing is used to estimate the state of the system. They can also be seen as an extension of holonomic visual servoing techniques to nonholonomic systems, with particular emphasis on recovering the robustness properties of these techniques, despite the highly nonlinear nature of the systems involved.

The associated experimental studies have been particularly important in both validating the existing theory, but also in demonstrating its weaknesses and in suggesting alternatives.

The further improvement of the robustness of these control schemes with respect to errors in modeling, timing and noise are some of the issues requiring additional research.

The papers [26], [27] and [28] can be found in the URL <http://www.ics.forth.gr/~tsakiris>.

References

- [1] J. Aloimonos and D.P. Tsakiris, “On the Visual Mathematics of Tracking”, *Image and Vision Computing* **9**, 235-251, 1991.
- [2] M.K. Bennani and P. Rouchon, “Robust Stabilization of Flat and Chained Systems”, *Proceedings of the 3rd European Control Conference (ECC)*, pp. 2642–2646, Rome, 1995.
- [3] R.W. Brockett, “Asymptotic Stability and Feedback Stabilization”, in *Differential Geometric Control Theory*, Eds. R.W. Brockett, R.S. Millman and H.J. Sussmann, Birkhauser, Boston, 1983.

- [4] J.-M. Coron, “Global Asymptotic Stabilization for Controllable Systems without Drift”, *Mathematics of Control, Signals and Systems* **5**, 295-312, 1992.
- [5] J.-M. Coron, “On the Stabilization in Finite Time of Locally Controllable Systems by Means of Continuous Time-Varying Feedback Law”, *SIAM J. Control and Optimization* **33**, 804-833, 1995.
- [6] A. DeLuca, G. Oriolo and C. Samson, “Feedback Control of a Nonholonomic Car-like Robot”, in *Robot Motion Planning and Control*, Ed. J.-P. Laumond, Lecture Notes in Control and Information Sciences, 229, Springer-Verlag, 1998.
- [7] B. Espiau, F. Chaumette and P. Rives, “A New Approach to Visual Servoing in Robotics”, *IEEE Trans. on Robotics and Automation* **8**, 313-326, 1992.
- [8] G.D. Hager and S. Hutchinson, Eds., “Vision-based Control of Robotic Manipulators”, Special section of *IEEE Trans. Robotics and Automation* **12**, 649-774, 1996.
- [9] K. Hashimoto, Ed., *Visual Servoing*, World Scientific, 1993.
- [10] H. Hermes, “Nilpotent and High-Order Approximations of Vector Field Systems”, *SIAM Review* **33**, 238-264, 1991.
- [11] B.K.P. Horn, *Robot Vision*, Mc Graw-Hill, 1986.
- [12] M. Kawski, “Homogeneous Stabilizing Feedback Laws”, *Control Theory and Advanced Technology* **6**, 497-516, 1990.
- [13] D. Lizarraga, P. Morin and C. Samson, “Non-Robustness of Continuous Homogeneous Stabilizers for Affine Control Systems”, INRIA Research Report RR-3508, 1998.
- [14] R.T. M’Closkey and R.M. Murray, “Exponential Stabilization of Driftless Nonlinear Control Systems Using Homogeneous Feedback”, *IEEE Trans. on Automatic Control* **42**, 614-628, 1997.
- [15] P. Morin and C. Samson, “Application of Backstepping Techniques to the Time-Varying Exponential Stabilization of Chained Form Systems”, INRIA Research Report No. 2792, Sophia-Antipolis, 1996
- [16] P. Morin and C. Samson, “Control of Nonlinear Chained Systems: From the Routh-Hurwitz Stability Criterion to Time-varying Exponential Stabilizers”, INRIA Research Report No. 3126, Sophia-Antipolis, 1997.
- [17] P. Morin, J.-B. Pomet and C. Samson, “Design of Homogeneous Time-Varying Stabilizing Control Laws for Driftless Controllable Systems via Oscillatory Approximation of Lie Brackets in Closed-Loop”, *SIAM J. Control and Optimization*, (1998) (To appear).
- [18] P. Morin and C. Samson, “Exponential Stabilization of Nonlinear Driftless Systems with Robustness to Unmodeled Dynamics”, *Control, Optimization and Calculus of Variations* **4**, 1-35, 1999 (Also available as INRIA Research Report No. 3477, Sophia-Antipolis, 1998).

- [19] N. P. Papanikolopoulos, P. K. Khosla and T. Kanade, “Visual Tracking of a Moving Target by a Camera Mounted on a Robot: A Combination of Control and Vision”, *IEEE Trans. Robotics and Automation* **9**, 14-35, 1993.
- [20] R. Pissard–Gibollet and P. Rives, “Applying Visual Servoing Techniques to Control a Mobile Hand–Eye System”, *IEEE Intl. Conf. on Robotics and Automation*, 1995.
- [21] J.–B. Pomet, “Explicit Design of Time–Varying Stabilizing Control Laws for a Class of Controllable Systems Without Drift”, *Systems & Control Letters* **18**, 147-158, 1992.
- [22] J.–B. Pomet and C. Samson, “Time–Varying Exponential Stabilization of Nonholonomic Systems in Power Form”, INRIA Research Report No. 2126, Sophia–Antipolis, 1993.
- [23] L. Rosier, “Homogeneous Lyapunov Functions for Homogeneous Continuous Vector Field”, *Systems & Control Letters* **19**, 467-473, 1992.
- [24] C. Samson, M. Le Borgne and B. Espiau, *Robot Control: The Task Function Approach*, Oxford University Press, 1991.
- [25] C. Samson, “Velocity and Torque Feedback Control of a Nonholonomic Cart”, in *Advanced Robot Control*, Ed. C. Canudas de Wit, Lecture Notes in Control and Information Sciences, No. 162, Springer-Verlag, 1990.
- [26] D.P. Tsakiris, K. Kapellos, C. Samson, P. Rives and J.–J. Borrelly, “Experiments in Real–time Vision–based Point Stabilization of a Nonholonomic Mobile Manipulator”, Preprints of the Fifth International Symposium on Experimental Robotics (ISER’97), pp. 463-474, Barcelona, Spain, June 15–18, 1997.
- [27] D.P. Tsakiris, P. Rives and C. Samson, “Applying Visual Servoing Techniques to Control Nonholonomic Mobile Robots”, Proceedings of the Workshop on “New Trends in Image–based Robot Servoing”, Eds. R. Horaud and F. Chaumette, IEEE/RSJ International Conference on Intelligent Robots and Systems (IROS’97), pp. 21-32, Grenoble, France, September 8-12, 1997.
- [28] D.P. Tsakiris, P. Rives and C. Samson, “Extending Visual Servoing Techniques to Nonholonomic Mobile Robots”, in *The Confluence of Vision and Control*, Eds. G. Hager, D. Kriegman and S. Morse, Lecture Notes in Control and Information Systems (LNCIS), Springer-Verlag, 1998.